Highly Sensitive SERS Detection of Neonicotinoid Pesticides. Complete Raman Spectral Assignment of Clothianidin and Imidacloprid

Highly Sensitive SERS Detection of Neonicotinoid Pesticides. Complete Raman Spectral Assignment of Clothianidin and Imidacloprid

Niamh Creedon[1], Pierre Lovera[1], Julio Gutierrez Moreno[2], Michael Nolan[2] and Alan O'Riordan[1]*

1: Nanotechnology Group, Tyndall National Institute, University College Cork, Lee Maltings, Cork, T12 R5CP, Ireland.

2: Materials Modelling for Devices Group, Tyndall National Institute, University College Cork, Lee Maltings, Cork, T12 R5CP, Ireland.

E-mail: alan.oriordan@tyndall.ie

Abstract:

The use of Surface Enhanced Raman Spectroscopy in the development of low cost, portable sensor devices that can be used in the field for nitroguanidine neonicotinoid insecticide detection is appealing. However, a key challenge to achieving this goal is the lack of detailed analysis and vibrational assignment for the most popular neonicotinoids. To make progress towards this goal, this paper presents an analysis of the bulk Raman and SERS spectra of two neonicotinoids, namely clothianidin and imidacloprid. Combined with first principles simulations, this allowed assignment of all Raman spectral modes for both molecules. To our knowledge, this is the first report of SERS analysis and vibrational assignment of Clothianidin and a comprehensive assignment and analysis is provided for imidacloprid. Silver nanostructured surfaces were fabricated for qualitative SERS analysis, which provides the characteristic spectra of the target molecules, and demonstrates the ability of SERS to sense these molecules at concentrations of 1 ng/mL. These concentrations are on a par with high-end chromatographic-mass spectroscopy laboratory methods. These SERS sensors thus allow for the selective and sensitive detection of neonicotinoids, and provides complementary qualitative data for the molecules. Furthermore, this technique can be adapted to portable devices for remote sensing applications. Further work focuses on integrating our device with an electronics platform for truly portable residue detection.

1. Introduction

The requirements for pest control in intensive agriculture systems has driven the growth of insecticide use within the agri-sector. In this regard, neonicotinoids are a relatively powerful class of insecticide. Imidacloprid was introduced in 1991 and the neonicitinoids have been the fastest-growing class of insecticides in modern crop protection,[1] taking *ca.* 17% of the global insecticide market.[2] Neonicotinoids target the nicotinic acetylcholine receptors in insects[3] and are extremely effective against herbivorous insects. The perceived low toxicity to mammals, birds and fish,[4] led to their widespread uptake for use on a variety of crops.

However recent years have seen significant concerns raised about the environmental impact of neonicotinoids on the global pollinator population, including honey bees, bumble bees and solitary bees. It is claimed that neonicotinoids affect the homing capacity of honey bees and their reproductive ability with the result of colony collapse disorder. [5-6] Another emerging concern is that human exposure to these pesticides may increase the prevalence of some cancers,[7-8] respiratory diseases [9-10] and damage to the reproductive system, nervous system and liver [11-12], while children are particularly at risk.[13] As a consequence, this class of insecticides has become the subject of a world-wide debate.[14-15] The European Food Safety Authority (EFSA), recognising the potential threat caused by neonicotinoids, enforced a temporary ban by the European Union in 2013.[16] The maximum allowable residue limits of neonicotinoids was set to between 0.01 and 3 mg/kg for many fruits and vegetables.[17-18] Ecological and human health risk assessments for selected neonicotinoids, Imidacloprid and Clothianidin were reviewed by the EFSA in 2018 and the assessment concluded that the use of neonicotinoid pesticides on outdoor crops presents a risk to wild bees and honeybees.[19] Consequently, in 2019, EU governments passed a near-total ban on the use of active neonicotinoid pesticides including clothianidin and imidacloprid on outdoor crops due to their impact on pollinators. To effectively enforce this ban the development of easy-to-use and low maintenance portable sensor devices is required to enable rapid and reliable decentralised detection of these pesticides.

Current techniques for the detection of neonicotinoids include both chemical and optical detection methods: enzyme linked immuno-sorbent assays (ELISA),[20-21] HPLC- or GC- mass spectrometry,[17, 22-25] voltammetric methods,[26-29] and fluorescence spectroscopy.[30] While these techniques can detect insecticides at low concentrations (low parts per billion), the associated instruments are complex, have a high cost of ownership and are cannot be used for remote field analysis. To permit rapid detection of these neonicotinoids in the field (*in situ*) necessitates the development of portable, low cost sensor devices. This can be realised using a single optical technique, namely surface enhanced Raman spectroscopy (SERS), which permits the necessary sensitive detection of the target species,

and trace analyte detection. Raman spectroscopy uses the vibrational properties of the compounds of interest, providing a spectral finger print of the molecule.[31-35] SERS enhancement occurs at nanostructured plasmonic surfaces following illumination with monochromatic radiation which arises from (i) an increase in local electromagnetic field strengths of localized surface plasmons (in nanogaps between metal clusters called "hot spots") and (ii) chemical resonant energy charge transfer In addition, SERS provides high sensitivity, rapid analysis time and little background interference from water molecules.

With this in mind, the present paper focuses on the development and use of SERS for the detection of the neonicotinoids clothianidin and imidacloprid as test cases for the wider application of SERS as a suitabledetection techniques for neonicotinoids. Bulk Raman studies were performed to explore the characteristic Raman modes to give a fingerprint for both molecules. A silver nanostructured polymer substrate was fabricated for SERS characterisation, which provides physical data (vibrational spectrum) for the insecticide solutions. Molecular identification was verified using SERS together with high level density functional theory simulations. This SERS sensor can be adapted for use in a single portable device. Integration into a portable device is beyond the scope of this paper which aims to demonstrate the ability of SERS to discriminate between the molecules of interest at very low concentrations (1 ng/mL) that are competitive with, or better than other technologies.

2. Experimental

2.1. Materials and Reagents

Polyvinylidene fluoride (PVDF), silver wire, imidacloprid and clothianidin were purchased from Sigma-Aldrich and used as received. Deionized water (18.2 MΩ cm) from an ELGA Pure Lab Ultra system was used for the preparation of samples.

2.2. SERS Substrate Fabrication

PVDF was selected as we have previously shown that the polymer exhibits superior adhesion to silver, compare to other polymers and very good optical transparency. Pellets of PVDF were placed on a microscope slide and melted on a hotplate at ~220°C. An aluminium (Al) master template was prepared as previously described by Creedon et al. [36]. The Al master was placed onto the melted droplet and pushed downward so the PVDF wetted the Al surface. The glass slide was removed from the hotplate and the PVDF was peeled from both the glass slide and Al template, to yield a

nanostructured polymer base. To complete the substrate fabrication, a thin silver layer (30 nm) was deposited onto the PVDF base by thermal evaporation (Edwards Autocore 500, 3×10^{-7} bar, ~1.6 A). The thickness and the deposition rate were controlled in situ using a calibrated quartz microbalance.

2.3. Microscopic and Raman Characterisation

Optical micrographs were acquired using a calibrated microscope (Axioskop II, Carl Zeiss Ltd.) equipped with a charge-coupled detector camera (CCD; DEI-750, Optronics). Scanning electron microscopy analysis was undertaken to characterize the SERS sensor surface after the fabrication procedure. SEM images were acquired using a calibrated field emission SEM (JSM-7500F, JEOL UK Ltd.) operating at beam voltages between 3 and 5 kV. All Raman measurements were recorded using a Confocal Renishaw Raman Microscope equipped with a 514 nm Ar ion laser and analysed using Wire 3.0 computer software. The laser spot diameter was ~1 μm at the substrate surface and a laser power density of ~7×10^4 W/cm^2 was used. SERS spectra collected using a 50x magnification (0.75 NA) objective microscope, with a data acquisition time of 10 s, over an extended spectral range of 200 cm^{-1} to 3500 cm^{-1}. The spectrometer was equipped with a computer controlled motorised XYZ stage employed to focus and adjust the positioning of the sample on the silver surface. Subtraction of the baseline was performed on all spectra to eliminate background noise from the underlying polymer and the recorded spectra were imported into Origin® 7.4 (OriginLab) to facilitate data analysis.

2.4. Computational Methodology

Density functional theory (DFT) calculations were undertaken to find the equilibrium molecular structures and aid the assignment of the Raman modes of the isolated imidacloprid and clothianidin molecules. The hybrid exchange-correlation functional B3-LYP, using Becke's three parameter exchange and Lee–Yang–Parr correlation [37] was used along with a triple-ζ valence basis set which has two sets of polarization functions, TVZPP [38]. These are implemented in the Turbomole 6.4 code.[39] The dispersion forces were corrected by the Grimme's DFT-D3 method.[40] Redundant internal coordinates were used for the geometry optimization with energy and gradient convergence criteria of less than 10^{-6} Hartree and 0.002 Hartree/Bohr. [41] Force constant calculations were implemented to estimate the vibrational modes of the isolated imidacloprid and clothianidin molecules and harmonic vibrational frequencies were estimated by the analytical evaluation of second derivatives of the energy.[42-43] A scaling factor of 0.9669 was applied to the fundamental vibrational frequencies to correct for the error due to the harmonic approximation in the theoretical model. [44]

2.5. Analysis of Neonicotinoids

Working solutions of both imidacloprid and clothianidin were prepared in a methanol– DI water solution (1:1) and diluted to 10 μg/mL and 1 ng/mL concentrations. Solutions were then deposited (50 μl) via a drop/dry process onto the SERS substrates (10 min). All samples were thoroughly rinsed with DI water before Raman analysis to remove unadsorbed, clumped molecules that accumulated on the surface of the substrate during the drying process. Bulk Raman spectra were also acquired for both molecules. In this work, all wavenumbers in the discussion section are related to the Raman spectra, unless otherwise stated.

3. Results and Discussion

3.1. SERS substrate Characterisation

A typical SEM micrograph of a portion of a fully prepared PVDF substrate, following Ag deposition, is shown in Figure 1. From SEM analysis the size distribution of the Ag nano-structures is estimated at 60 ± 20 nm while the gaps between the clusters are *ca.* 10 ± 5 nm. The small separation between Ag clusters delivers a high yield of electromagnetic hot-spots, making them very attractive and suitable for SERS sensing. A model compound, crystal violet, was analysed to characterise the SERS capabilities of the substrate and the results of this characterisation are presented in Supp. Info (Figure S1), while further substrate characterisation was explored in significant detail [36] These substrates demonstrated high sensitivity to crystal violet yielding enhancement factors of ~10^6. In previous work, we have shown that the nanostructured surface is 3D in nature, and this topography is required to yield a SERS response from the substrate. No SERS response was observed for CV on planar (non-structured) silver substrates Ref. (35).

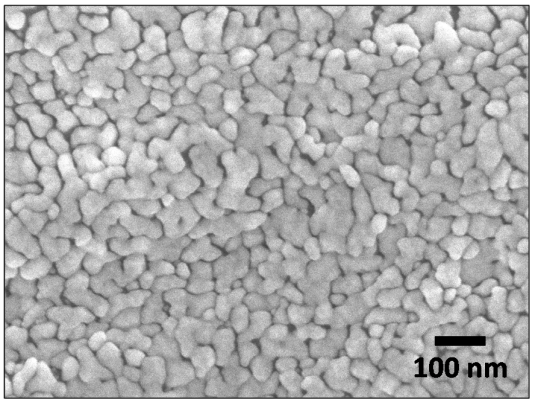

Figure 1: SEM image of a portion of the fabricated SERS substrate silver surface.

3.2. Raman and SERS Analysis of Clothianidin

Bulk Raman spectra were first acquired for Clothianidin and the Raman spectrum is shown in Figure 2a, exhibiting all the expected characteristic peaks of this molecule. Clothianidin consists of a chloro-thiazole ring linked by a carbon to a nitroguanidine structure. The strongest Raman peaks were identified and assigned to their corresponding vibrational modes by visualization of the vibrational modes from the DFT calculations and comparison to the corresponding vibrations in similar molecules in the literature[45-46] and the assignments are shown in Table 1. In general, the scaled DFT frequencies for the vibrational modes are in good agreement with the experimental vibrational frequencies. The full set of Raman assignments for Clothianidin are discussed in detail in the Supporting Information (SI, Section S2). Although we did not model the explicit interaction of the target molecules with silver surfaces as the focus of the modelling was on the assignment of the Raman modes, we expect from previous work, that the interaction is physisorption or weak chemisorption, as the Raman spectra indicate that molecules are not dissociated or strongly distorted [47]. We note that here are some spectral differences in the peaks observed in Figure 2a and Figure 2b where there is a change in relative intensities and/or a shift in wavelength. We speculate that these are due to how the molecule attaches to the surface. Adsorption of the molecules is known to change the energy of the molecule and disrupt the vibrational modes, thus shifting peaks and increasing or decreasing peak intensities [48]. The structure of clothianidin together with the atomic numbering used in the later discussion is given in Figure 2c.

C-H vibrations

The C-H stretching vibrations observed in the spectral range from ~3000 - 3600 cm^{-1} are presented in Table S1 (SI, Section 2) and we discuss the most relevant modes here. The Raman band at 3121 cm^{-1} is assigned to the C-H stretch in the chlorothiazole ring, C13-H19. There are in-plane bending vibrations associated with C13-H at 1532 cm^{-1}, 1296 cm^{-1}, 1248 cm^{-1} and 1152 cm^{-1}. The out of plane wagging modes for C13-H are observed at 871 cm^{-1} and 669 cm^{-1}. The C10-H symmetric and asymmetric stretching modes are observed at 2965 cm^{-1} and 3011 cm^{-1}, respectively and the bending mode is at 1462 cm^{-1}. Multiple out of plane twisting modes were found at 1422 cm^{-1}, and 1051 cm^{-1}. Finally, Raman bands at 947 cm^{-1}, 669 cm^{-1} and 259 cm^{-1} can be assigned to the in-plane rocking of H16 and H17 with C10. The methyl C-H symmetric and asymmetric stretching modes are observed at

2860 cm^{-1} and 2900 cm^{-1}, respectively, while the in-plane bending and wagging modes of methyl are found at 1422 cm^{-1} and 992 cm^{-1}.

Ring Vibrations

C-C and N-C stretching modes are found at at 1532 cm^{-1} and 1433 cm^{-1} and can be assigned to ring C13-C11 and N7-C14 bonds. A strong asymmetric stretch between C14-S2, Cl1 is assigned to the 992 cm^{-1} band. The observed band at 594 cm^{-1} is assigned to the out of plane wagging modes of the chlorothiazole ring and other out-of-plane wagging modes are at 443 cm^{-1} and 358 cm^{-1}. The stretching vibrational mode for the C14-Cl1 bond is seen at 432.6 cm^{-1} in the SERS spectra and is agreement with the literature data.[49] Raman peaks at 259 cm^{-1} and 358 cm^{-1} are assigned to the weak bending and wagging mode of C-Cl, respectively.

N-O, N-H and C-N Vibrations

The N9-O symmetric and asymmetric stretching vibrations occur at 1318 cm^{-1} and 1570 cm^{-1}, respectively, which are typical for nitroalkane stretching as reported in the literature.[49-50] The wagging out of plane vibration of N9-O appears at 754 cm^{-1}; while the N9-O rocking occurs at 358 cm^{-1}. There is a strong N9-N6 stretching mode at 992 cm^{-1} and a C12-N6 stretch at 1152 cm^{-1}.

The C12-N wagging mode is found at 669 cm^{-1} and the C12-N bending mode is observed at 1318 cm^{-1}. The N8-C15 stretching modes are found at 651 cm^{-1}, 947 cm^{-1} and 1051 cm^{-1}. The Raman band at 310 cm^{-1} shows a bending mode involving N5, C12 and O4. Similar bending and wagging vibrations are also seen at 443 cm^{-1}. The out of plane N-H wagging vibrations (N6H20 and N5H18) are observed at 651 cm^{-1}, 514 cm^{-1} and 577 cm^{-1}. The in-plane N-H bending modes are observed at 1051, 1248, 1318, 1422 and 1532 cm^{-1}.

SERS of Clothianidin

The SERS of clothianidin solutions was investigated using our SERS substrates. Figure 2b shows the SERS spectra ~~for~~ (10 μg/mL) of clothianidin. The major peaks are well resolved and the large characteristic peaks compare well to the bulk Raman spectrum. These SERS peaks were matched to the Raman active vibrational modes assigned in Table 1. We expect a shift in wavenumber for the SERS peaks for a solution compared to the bulk Raman spectrum. This is due to the adsorption of clothianidin to the SERS substrate Ag surface via nitrogen atoms in the nitroguanidine structure. The largest shifts in the vibrational modes of the SERS spectra were for those modes involving the atoms in the nitroguanidine moiety. This is typical when employing surface enhanced Raman techniques.

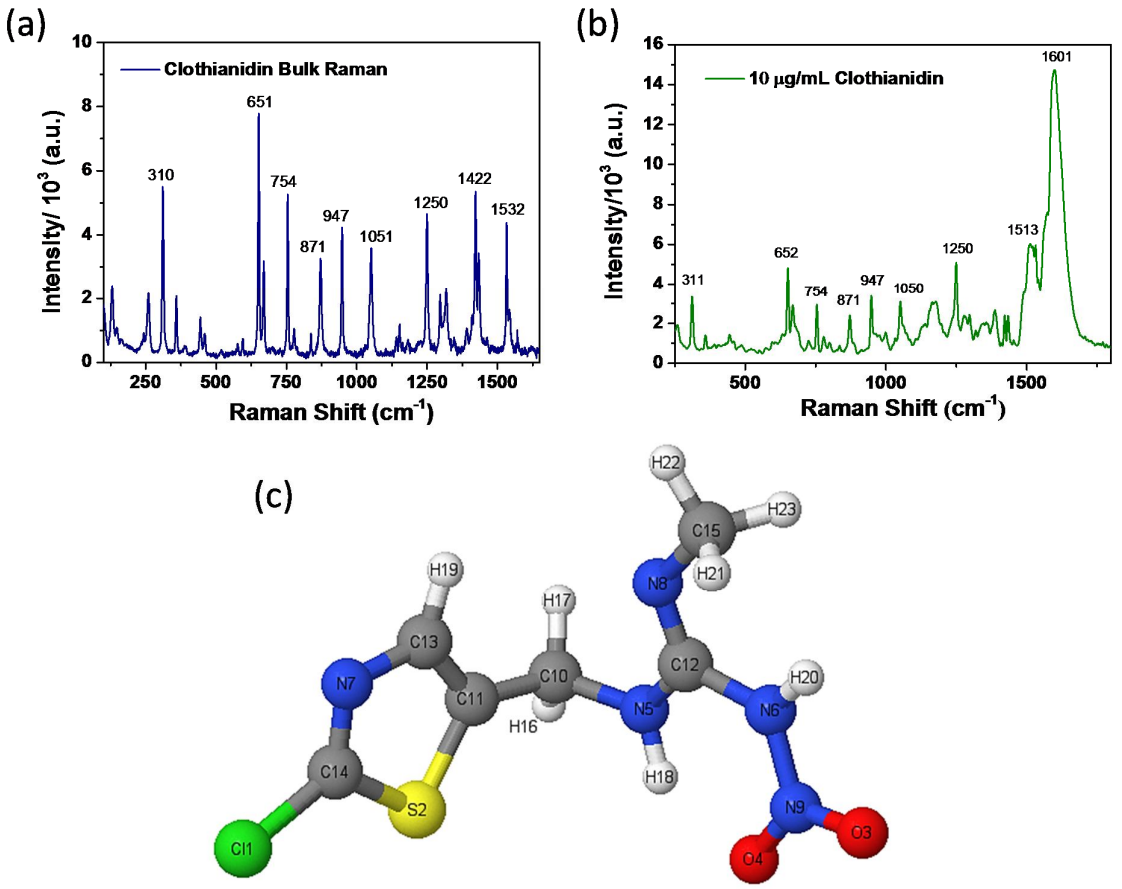

Figure 2: (a) Bulk Raman spectrum and (b) SERS spectrum (10 µg/mL) of clothianidin using fabricated silver coated PVDF substrates. (c) Atomic structure of Clothianidin with atomic numbering.

Raman / cm^{-1}	SERS (1ng) / cm^{-1}	DFT (scaled) / cm^{-1}	Mode Assignments
1570	1605	1669/1604	νN9O3O4 as; δN6H20; δN5H18
1532	1557	1517.25	νC11C13; νC10C11; δC13H19 (ip); δN5H18; νN7C14;
1433		1413.35	νN7C14; νC11C13; τC10H17,18
1422	1423	1403	δC15H21-23; δN6H20
1318	1335	1317	νN6N9; νN9O3,4 sym; δN8C12N5N6 ; δC5H18 (ip); ωC10H16 (oop)
1296	1304	1297	δC10C11C13; τC10H16,17 (oop); δC13H19
1248	1254	1237	τ C10H16,17 (oop); δC13H19 (ip); δN6H18; δC6H20
1152	1176	1148/1126	νC10C11; ρC10H16,17 (ip); δC13C11C10; νC11S2; νN6C12; δC13H19 (ip); νC13N7

1051	1047	1051.46	νHC15N8; νC10N5; δN5H18 (ip); τC10H16,17 (oop);
992	997	997.65	νN15N19; νN9O3O4 sym; ωC15H21-24; νC14S2Cl1 as; δN7C14C13H19
947	946	931.8	ρC10H16,17 (ip); δN5H18 (ip); νC15N8; δC10C11C13
871		867.64	ωC13H19 (oop)
754	758	750.01	ωN6N9O3O4
669		678	ωC12N5N6N8; ωC12N5C10C11; ρC10H16,17; νS2C11C14 as; ωC13H19
651	650	671.83	δN5C12C10H; ωN5H18 (oop); νS2C11C14 sym; νHN6N9O3; νN8C15
594	573	589	ωC10C11C13; ωHC13N7C14; ωC11C13N7C14; ωC13N7C14Cl1
577	556	545.78	ωN6H20; ωN5H18; ωS2C11C14; νC14Cl1
514	522	514	ωN6H20; ωN5H18
443	432	453	ωC11C13N7C14; ωH19C13N7C14S2; νC14Cl1; ωC12N5H18C10; δN6N9O3;
358	358	339.41	ρN9O3O4; ωC13N7C14Cl1; ωC14Cl1; ωHC10; δC12N6N9; ωC10C11S2; ωC12N5C10C11
310	310	292.69	δC12N6N9O4; δN6C12N8C15H; ωC12N5H18C10; δS2C14Cl1
259	238	237.97	ρC10H16,17; δS2C14Cl1; δN8C15H

Table 1: Raman assignations for Clothianidin. The abbreviations are ν, stretching; ω, wagging; τ, twisting; ρ, rocking; δ, bending/scissoring; ip, in plane and oop, out of plane modes. sym and asym denote symmetric and asymmetric modes, respectively.

3.3. Raman and SERS Analysis of Imidacloprid

Figure 3 shows the bulk Raman spectrum for Imidacloprid and the SERS detection (10 μg/mL solution) in Figure 3a and Figure3b, respectively. The imidacloprid molecule consists of a chloropyridine ring linked with a carbon to an imidazole ring structure. For the purpose of assigning the Raman modes, we name these structures, ring 1 and ring 2, respectively. The structure of imidacloprid, with the atomic numbering used is shown in Figure 3c. We again note that here are some spectral differences in the peaks observed in Figure 3a and Figure 3b where there is a change in relative intensities and/or a shift in wavelength. We again speculate that these are due to how the molecule attaches to the surface. Adsorption of the molecules is known to change the energy of the molecule and disrupt the vibrational modes, thus shifting peaks and increasing or decreasing peak intensities. [48]

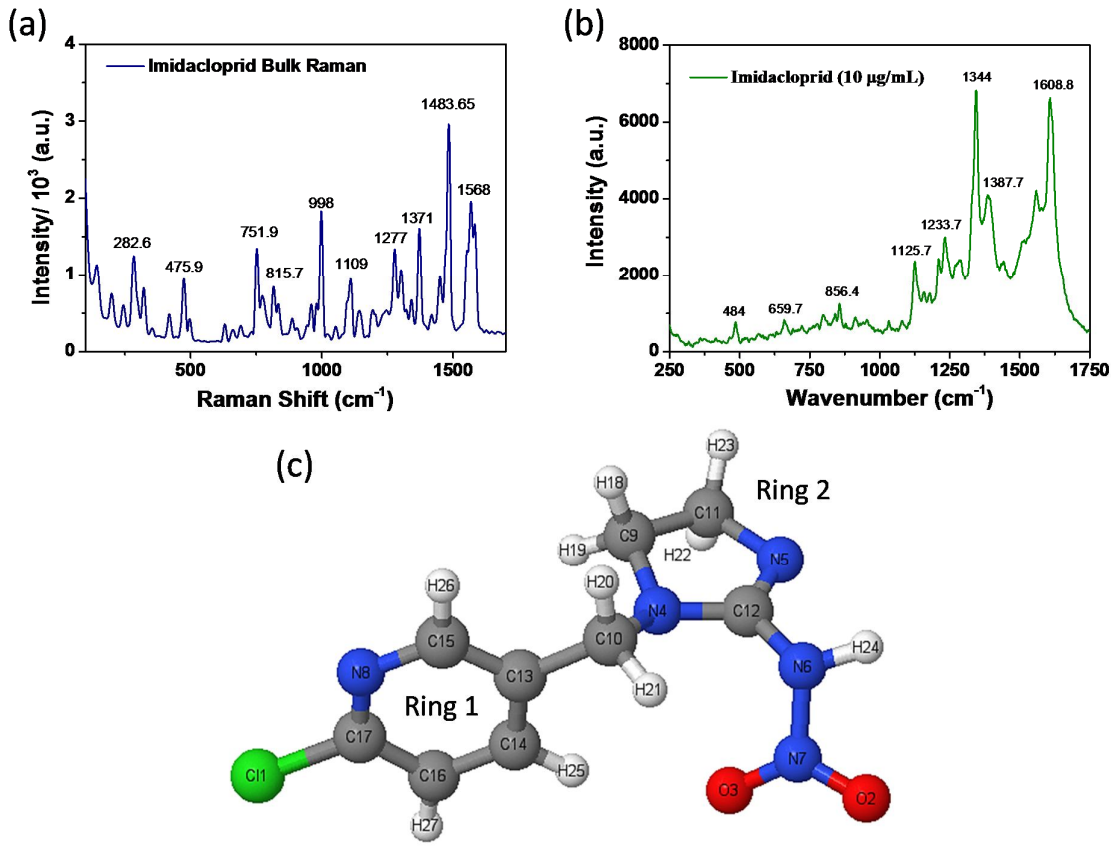

Figure 3: (a) Bulk Raman spectrum and (b) SERS spectrum (10 µg/mL) of imidacloprid using fabricated silver coated PVDF substrates. (c) Structure of imidacloprid with atomic numbering.

The assignments of the key Raman modes are summarised below, and in detail in the SI (Section S3). The Raman spectrum was compared with the SERS spectrum and the DFT results and the assignments are presented in Table 2. [51-53] Similar to clothianidin, the adsorption of imidacloprid to the SERS substrate will be expected to shift some Raman modes. Typically for molecules that contain a pyridine ring, attachment to the metal surface is via N in pyridine. [54] We expect that the largest shifts the SERS spectra will be observed with Raman vibrational frequencies relating to Ring 1. This is again due to the adsorption of imidacloprid to the SERS substrate Ag surface via nitrogen atoms in the nitroguanidine structure.

Raman / cm^{-1}	SERS / cm^{-1}	DFT (Scaled) / cm^{-1}	Vibrational Assignments

1584	1607	1632/ 1606	νC12N4N5N6 as; δN6H24; νN7O2O3 as
1568	1568	1575/1547	CCC Stretching: νC13C14C15 as; νC17N8C16 as
1483	1464	1483.3	δC9H19,H18; δC11H23,H22
1451		1448.909319	νC16C17C14 as; νC17N8; δHC14; δHC15; δHC16; δC10H20,H21
1371	1387	1376	νC16C17C14 sym; νC15N8C13 sym; ωC10H20H21
1302	1334	1320/1282	ωC9H19H18; ωC11H22H23; ωC10H20H21; δC14H25; νN7O2O3 sym
1277	1327	1279.75	νN7O2O3 sym; ωC9H1918; τC11H22H23; τC10H20H21; δHC15; δHC16
1241	1298.	1253.77	Ring 1 stretching; τC10H20H21; ωC9H1918; ωC11H22H23; νC12N4N5N6 as; νN6N7
1195	1233	1217.61	τC9H18H19; τC11H22H23
1142	1190	1197	νC10C13; νC10C13C14C15 as; ωC10H20; ωC14H25; ωC15H26; ωC16H27;
1109	1125	1125.97	δH25C14C16H27; νC14C16;
998	987	1008.09	δC17C16N8; δC13C14C15
815	856	815.11	δC17C16N8, νC13C14C15C10 sym; νC17Cl1; ρC9H18H19; ρC11H23H24
751	740	768.22	O3O2N7N6 oop; Ring 2 breathing: [δN6N7C12, δC11N5C9]; ρC11H22H23; ρC9H18H19; δC10N4C13
691	677	683	C12N4N5N6 oop; ρC9C11-H sym; δC10N4; Ring 1 breathing: [δC10C14C15, νC17Cl1]
660	661	662/654	ωC12N4N5N6 oop; δC9C11N4; νC13C14C15; νC17Cl1; δC10N4C13
631	635	622	δN8C17C15; δC14C13C16; δC12N4C9C11
475	484	453	Ring 2 rocking: [ρC10N4C12N6 ρN6C12N4N5] δC13C10N4C12; νC17Cl1; ωC13C14C15; τN8C17C15;
320	320	306	ωN4C12N5; δN4C10C9 oop, δC12N5N16]; δC12N6N7O3
282	282	274	ρC10H20H21; ρC11H22H23; δC17Cl1
142	133	144.91	δN6N7O3; ρC11H22H23; ρC10C13N4

Table 2: Raman and SERS assignations for imidacloprid. The abbreviations are ν, stretching; ω, wagging; τ, twisting; ρ, rocking; δ, bending/scissoring; ip, in plane and oop, out of plane modes sym and asym denote symmetric and asymmetric modes, respectively.

C-H vibrations

The stretching modes for C14, C15 and C16 C-H bonds are visible in the extended spectral range at frequencies above ~3000 cm^{-1} , see Figure S4 in the SI, which is typical for C-H hetero-aromatic stretching vibrations.[55] The in-plane bending vibrations are observed at 1451 cm^{-1}, 1371 cm^{-1} and 1277 cm^{-1}while out of plane wagging modes for the pyridine ring (ring 1) are observed at 1142 cm^{-1}.

Raman modes at 2951 cm^{-1} and 2970 cm^{-1} correspond to C-H symmetric and asymmetric stretching modes involving C9H and C11H. The strong in plane bending vibration for C9-H and C11-H appears as at 1484 cm^{-1}. A twisting vibrational mode was also observed at 1195 cm^{-1}. Finally, multiple C9-H and C11-H in-plane rocking modes were observed at 815 cm^{-1}, 751 cm^{-1}, 691 cm^{-1} and 142 cm^{-1}. The C10 symmetric stretching modes with H21 and H20 were observed at 3008 cm^{-1} and 2878 cm^{-1}, respectively. The only C10H bending vibration is found at 1451 cm^{-1}.

Ring Vibrations

Raman modes at 1568 cm^{-1}, 1451 cm^{-1} and 1371 cm^{-1} are attributed to two asymmetric and one symmetric stretching modes in ring 1. Other stretching modes in Ring 1 are observed at 1142 cm^{-1} and 815 cm^{-1}.

The peaks at 998 cm^{-1} and 691 cm^{-1} are attributed to weak ring bending vibrations in Ring 1. Finally, the Raman peak at 631 cm^{-1} arises from a strong symmetric bending mode of C14 with C13/ C16 and N8 with C15/ C17. The Raman band at 476 cm^{-1} is attributed to wagging of C13 and C17 atoms out of plane in ring 1.

Due to the orientation of imidacloprid, the majority of the imidazole ring vibrational modes (ring 2) are observed as out-of plane vibrations. In-plane rocking and breathing modes are observed at 475 cm^{-1} and 751 cm^{-1}, respectively. The 320 cm^{-1} band is assigned as a ring wagging. A strong C12-N asymmetric stretch is observed at 1584 cm^{-1} and a weaker asymmetric stretch is at 1241 cm^{-1}. The common C12-N wagging vibrations are at 691 cm^{-1} and 660 cm^{-1}.

N-O and C-N Vibrations

The N7-O symmetric and asymmetric stretching vibrations occur at 1302 cm^{-1}[11] and 1584 cm^{-1}, respectively. These are two well resolved bands in both the Raman and SERS spectra, and compare well to the nitroalkane stretching mode reported in the literature.[55] The out of plane wagging vibration of N7-O is observed at 751 cm^{-1}; while the bending vibration of N6-N7-O2-O3 occurs at 142 cm^{-1}. The

N6-N7 stretching mode is observed at 1241 cm^{-1}, with a second strong stretching mode at ~1050 cm^{-1}. A strong in-plane N6N7O2 bending mode is seen at 443 cm^{-1}.

3.4. SERS Detection of Neonicotinoids

Having demonstrated that SERS is able to discriminate the presence of our target neonicotinoids at high concentrations, we explore the use of SERS for the qualitative detection of clothianidin and imidacloprid in solution at low concentrations that are relevant for the allowed concentrations of neonicitinoids, and we show SERS detection down to 1 ng/mL. The SERS spectrum of clothianidin is shown in

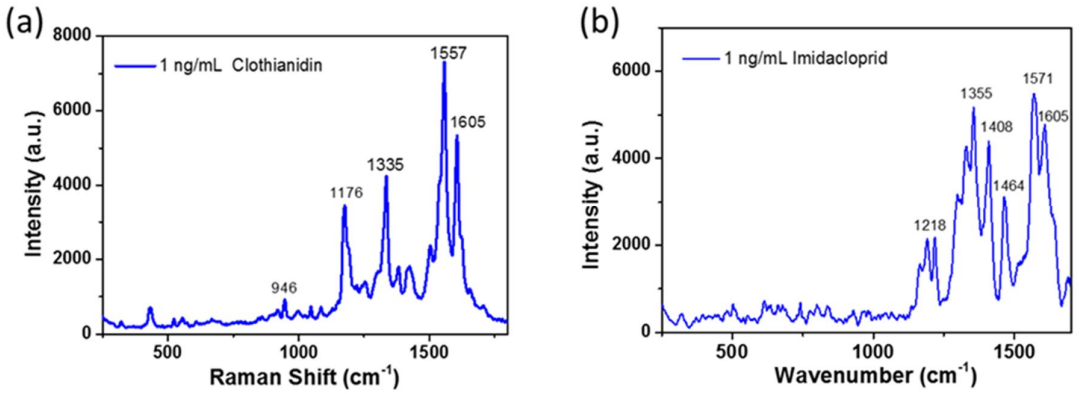

Figure 4a.

Although the Raman peaks are not particularly well resolved or strong at below 940 cm^{-1}, there are clear strong peaks at 946, 1176, 1335, 1557 and 1605 cm^{-1}, which correspond to the previously established characteristic peaks of clothianidin at 947, 1152, 1318, 1532 and 1570 cm^{-1} in the Raman spectrum. These peaks therefore act as a fingerprint for the presence of clothianidin in solution. This finding demonstrates that clothianidin can be detected by our SERS sensors at these previously unreachable concentrations using a simple drop and dry method.

In a similar manner, the SERS spectrum for a solution of 1 ng/mL of imidacloprid is presented

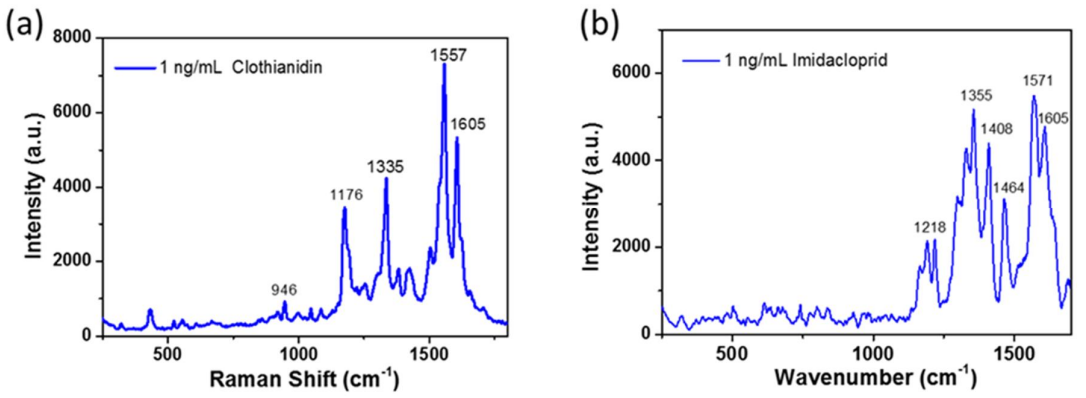

Figure 4b. Again the peaks at high wavenumbers, beyond 1200 cm^{-1} which correspond to the characteristic peaks of the molecule, are well resolved. Bands at 1218, 1355, 1408, 1464, 1571 and 1605 cm^{-1}, labelled in

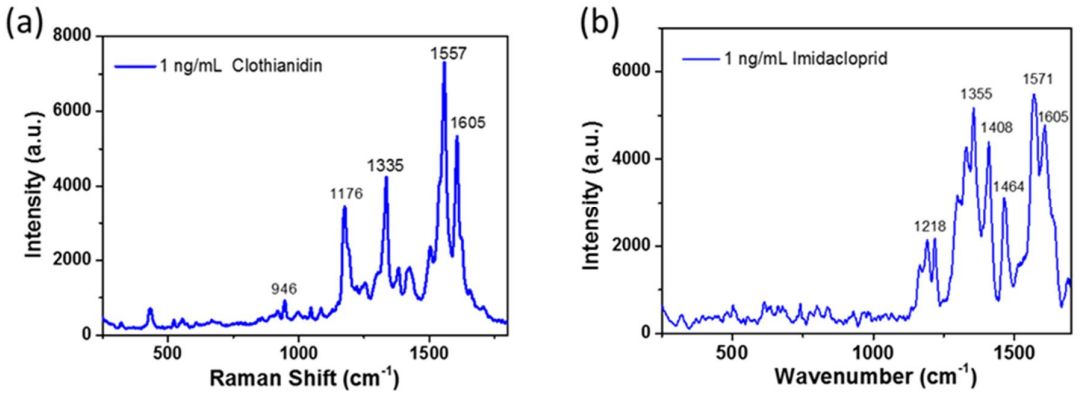

Figure 4b, are similar to those in the bulk Raman spectrum (refer back to Figure 2a). They are mainly attributed to the bending and wagging of the ring structures in imidacloprid. A key result is that minimum detection concentration that we achieved is significantly lower than the current lowest legal residue limit of *ca.* 10 ng/mL for food products [56] which demonstrates the power of SERS technique for the detection of neonicotinoid residues.

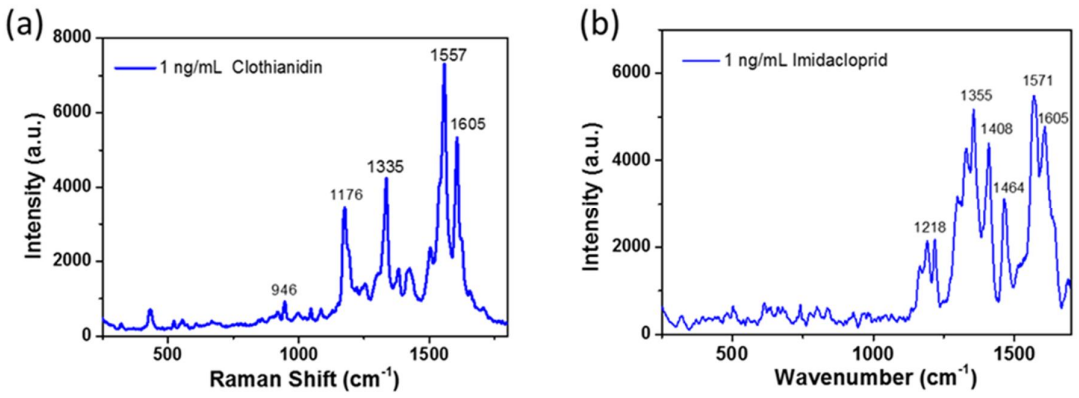

Figure 4: SERS detection of (a) clothianidin and (b) imidacloprid at 1 ng/mL using the fabricated silver coated PVDF substrates.

Comparing Figure 4a with Figure 2b, at 1 ng/mL, peaks at 1176, 1335, and 1557 cm^{-1} are very large and clear in Figure 4a, but at 10 µg/mL, these peaks are very hard to identify. This is especially evident for the 1557 cm^{-1} peak, which is the largest peak in Figure 4a, but it is hard to identify in Figure 2b. to explain this, we and others have observed that the concentration of an analyte influences the intensities of the observed peaks – this is a key reason why quantitative measurements with Raman spectroscopy is difficult [48]. A reproducible dependence of the SERS intensity on the analyte concentration can only be obtained for a certain dynamic range which appears to be dependent on what molecule is being measured, the plasmonic metal being used (and how it is prepared) and the nature of the hotspots. This deviation from the low-concentration relation between SERS intensity and concentration is assumed to be due to the influence of the adsorption geometry, which becomes important if the amount of adsorbant increases. In SERS, there is the additional complication of the orientation of the molecule on the surface. All this can change the selection rules for Raman and will lead to some vibrations being enhanced, some disappearing and some shifting. Specially in the drop and dry method as described in this paper. If the concentration is high, it is possible that at the 10 µg/mL molecules will tend to recrystallize upon drying. Therefore, the SERS for higher concentration could/would be an enhancement of the bulk (i.e. small crystals trapped in hot spots), and the observed SERS spectrum will be closer to the bulk one. When concentration decreases, then SERS more likely to be single or few molecules, and therefore bigger changes vs bulk Raman (compounded by orientation). Furthermore, it must be noted that the intensities are stated in arbitrary units and since each substrate has variations in density of hot spots, some sections may provide a higher response to others.

3.5. Comparison with other Techniques

The results for neonicotinoid detection obtained using our nanowire array SERS devices are compared against literature reports and Table 3 presents typical limits of detection. The measured limit of detection for the present SERS devices is a significant improvement over solid state electrochemical measurements and on a par with results achieved using high-end laboratory instrumentation, but with the advantage of low cost and potential in situ use of the sensor devices. The use of SERS to detect the presence of these neonicotinoids gives a very useful, accurate, and potentially *in-situ*, analytical tool and clearly demonstrates the viability of this approach to the selective detection of neonicotinoid species.

Detection method	Electrode Type/ Diameter	Neonicotinoid	LOD	Ref
Enzyme-linked immunosorbent assays	-	Imidacloprid	20 nM	20
	-	Clothianidin	11 nM	57
Gas Chromatography – Mass Spectroscopy	-	Clothianidin	40 nM	28
Tandem Mass Spectrometry	-	Clothianidin	40 nM	58
High performance liquid chromatography	-	Imidacloprid	90 nM	59
	-	Imidacloprid	39 nM	60
	-	Clothianidin	10 nM	61
Differential-Pulse Voltammetry	Bismuth-Film Modified GCE	Clothianidin	3000 nM	62
	Carbon paste electrode (d = 2 mm)	Imidacloprid	2030 nM	59
	Hanging Mercury drop electrode	Imidacloprid	2560 nM	63
	Nanosilver/SDS GCE (d = 3 mm)	Imidacloprid	250 nM	64
	Hanging Mercury drop electrode	Imidacloprid	39 nM	65
Cyclic voltammetry	Glassy carbon Electrode (GCE)	Imidacloprid	10.9 μM	27
	Nanosilver/SDS GCE (d = 3 mm)	Imidacloprid	630 nM	64
	Reduced graphene oxide GCE (d = 3 mm)	Imidacloprid	400 nM	66
Square wave Voltammetry	Silver-Amalgam Film Electrode	Clothianidin	2080 nM	67
	Hanging Mercury drop electrode	Imidacloprid	16 nM	26
Surface Enhanced Raman Spectroscopy (SERS)		Imidacloprid	19.5 nM	68
		Imidacloprid	40 nM	69
		Clothianidin	Not reported previously	
		Imidacloprid	**4 nM**	**This**
		Clothianidin	**4 nM**	**work**

Table 3: Comparison of detection methods for clothianidin and imidacloprid in the literature compared with our results.

4. Conclusion

The use of Surface Enhanced Raman Spectroscopy in the development of low cost, portable sensor devices that can be used in the field for nitroguanidine neonicotinoid insecticide detectionis appealing. To make progress towards this goal, this paper presents an analysis of the bulk Raman and SERS spectra of two neonicotinoids, namely clothianidin and imidacloprid, together with the use of SERS to demonstrate the sensing of these molecules.

Silver nanostructured surfaces were fabricated for qualitative SERS, which provides the characteristic spectra of the target molecules. Combined with first principles simulations, this allowed assignment of all Raman spectral modes for both molecules. To our knowledge, this is the first report of SERS analysis and vibrational assignment of Clothianidin and we demonstrate SERS detection neonicotinoid insecticide at concentration s as low as 1 ng/mL.

These measured detection concentrations are significantly lower than reported solid state electrochemical techniques and are on par with high-end chromatographic-mass spectroscopy laboratory methods. These SERS sensors thus allow for the selective and sensitive detection of neonicotinoids and provides complimentary qualitative data for the molecules. Furthermore, this technique can be adapted to portable devices for remote sensing applications. Further work focuses on integrating our device with an electronics platform for truly portable residue detection. Future work will focus on translating this method to samples with complex matrices. As neonicotinoids are banned in Ireland, we cannot test real samples, but we intend to use these substrates to test spiked river water/ farm run off for neonicotinoids. Principal component analysis methods will be employed to de-convolute spectra obtained from complex matrices.

Supporting Information

The Supporting Information is available free of charge at https://pubs.acs.org/doi/10.1021/acs.xxxxx.

SERS sensor Characterisation with Crystal Violet, full Clothianidin vibrational analysis, full imidacloprid vibrational analysis (PDF).

5. Acknowledgments

This publication has emanated from research supported in part by a research grant from Science Foundation Ireland (SFI) under Connect (13/RC/2077), the VistaMilk Centre Science Foundation Ireland (SFI); Department of Agriculture Food and the Marine (DAFM) under Grant Number 16/RC//3835, the Technology Innovation Development Award (SFI/12/TIDA12377) and Environmental Protection Agency UisceSense (EPA 2015-W-MS-21)

6. References

1. Elbert, A.; Haas, M.; Springer, B.; Thielert, W.; Nauen, R., Applied aspects of neonicotinoid uses in crop protection. *Pest Management Science* **2008,** *64* (11), 1099-1105.
2. Jeschke, P.; Nauen, R., Neonicotinoids—from zero to hero in insecticide chemistry. *Pest Management Science* **2008,** *64* (11), 1084-1098.
3. Nauen, R.; Bretschneider, T., New modes of action of insecticides. *Pesticide Outlook* **2002,** *13* (6), 241-245.
4. Tomizawa, M.; Casida, J. E., Neonicotinoid insecticide toxicology: mechanisms of selective action. *Annual Review of Pharmacology and Toxicology* **2005,** *45*, 247-268.
5. Henry, M.; Beguin, M.; Requier, F.; Rollin, O.; Odoux, J.-F.; Aupinel, P.; Aptel, J.; Tchamitchian, S.; Decourtye, A., A common pesticide decreases foraging success and survival in honey bees. *Science* **2012,** *336* (6079), 348-350.
6. Whitehorn, P. R.; O'Connor, S.; Wackers, F. L.; Goulson, D., Neonicotinoid pesticide reduces bumble bee colony growth and queen production. *Science* **2012,** *336* (6079), 351-352.
7. Miligi, L.; Costantini, A. S.; Veraldi, A.; Benvenuti, A.; Will; Vineis, P., Cancer and Pesticides. *Annals of the New York Academy of Sciences* **2006,** *1076* (1), 366-377.
8. Meinert, R.; Schüz, J.; Kaletsch, U.; Kaatsch, P.; Michaelis, J., Leukemia and non-Hodgkin's lymphoma in childhood and exposure to pesticides: results of a register-based case-control study in Germany. *American Journal of Epidemiology* **2000,** *151* (7), 639-646.
9. Betarbet, R.; Sherer, T. B.; MacKenzie, G.; Garcia-Osuna, M.; Panov, A. V.; Greenamyre, J. T., Chronic systemic pesticide exposure reproduces features of Parkinson's disease. *Nature Neuroscience* **2000,** *3* (12), 1301-1306.
10. Salameh, P.; Baldi, I.; Brochard, P.; Raherison, C.; Saleh, B. A.; Salamon, R., Respiratory symptoms in children and exposure to pesticides. *European Respiratory Journal* **2003,** *22* (3), 507-512.
11. Kimura-Kuroda, J.; Komuta, Y.; Kuroda, Y.; Hayashi, M.; Kawano, H., Nicotine-like effects of the neonicotinoid insecticides acetamiprid and imidacloprid on cerebellar neurons from neonatal rats. *PloS one* **2012,** *7* (2), e32432.
12. Duzguner, V.; Erdogan, S., Acute oxidant and inflammatory effects of imidacloprid on the mammalian central nervous system and liver in rats. *Pesticide Biochemistry and Physiology* **2010,** *97* (1), 13-18.
13. Hanke, W.; Jurewicz, J., The risk of adverse reproductive and developmental disorders due to occupational pesticide exposure: an overview of current epidemiological evidence. *International Journal of Occupational Medicine and Environmental Health* **2004,** *17* (2), 223-243.
14. Blacquiere, T.; Smagghe, G.; van Gestel, C. A.; Mommaerts, V., Neonicotinoids in bees: a review on concentrations, side-effects and risk assessment. *Ecotoxicology* **2012,** *21* (4), 973-92.
15. Wood, T. J.; Goulson, D., The environmental risks of neonicotinoid pesticides: a review of the evidence post 2013. *Environmental Science and Pollution Research* **2017,** *24* (21), 17285-17325.
16. European Commission, Commission Implementing Regulation (EU) No 485/2013 of 24 May 2013 amending Implementing Regulation (EU) No 540/2011, as regards the conditions of approval of the active substances clothianidin, thiamethoxam and imidacloprid, and prohibiting the use and sale of seeds treated with plant protection products containing those active substances. *Official Journal of the European Union* **2013,** *139*, 12-14.
17. Ferrer, I.; Thurman, E. M.; Fernández-Alba, A. R., Quantitation and Accurate Mass Analysis of Pesticides in Vegetables by LC/TOF-MS. *Analytical Chemistry* **2005,** *77* (9), 2818-2825.
18. European Food Safety Authority, The 2014 European Union Report on Pesticide Residues in Food. *EFSA Journal* **2016,** *14* (10), e04611-n/a.

19. European Food Safety Authority, Peer review of the pesticide risk assessment for bees for the active substance clothianidin considering the uses as seed treatments and granules. *EFSA Journal* **2018,** *16* (2), e05177.
20. Lee, J. K.; Ahn, K. C.; Park, O. S.; Kang, S. Y.; Hammock, B. D., Development of an ELISA for the Detection of the Residues of the Insecticide Imidacloprid in Agricultural and Environmental Samples. *Journal of Agricultural and Food Chemistry* **2001,** *49* (5), 2159-2167.
21. Watanabe, E.; Baba, K.; Eun, H.; Miyake, S., Application of a commercial immunoassay to the direct determination of insecticide imidacloprid in fruit juices. *Food Chemistry* **2007,** *102* (3), 745-750.
22. Obana, H.; Okihashi, M.; Akutsu, K.; Kitagawa, Y.; Hori, S., Determination of Acetamiprid, Imidacloprid, and Nitenpyram Residues in Vegetables and Fruits by High-Performance Liquid Chromatography with Diode-Array Detection. *Journal of Agricultural and Food Chemistry* **2002,** *50* (16), 4464-4467.
23. Liu, S.; Zheng, Z.; Wei, F.; Ren, Y.; Gui, W.; Wu, H.; Zhu, G., Simultaneous Determination of Seven Neonicotinoid Pesticide Residues in Food by Ultraperformance Liquid Chromatography Tandem Mass Spectrometry. *Journal of Agricultural and Food Chemistry* **2010,** *58* (6), 3271-3278.
24. Aguera, A.; Almansa, E.; Malato, S.; Maldonado, M.; Fernandez-Alba, A., Evaluation of photocatalytic degradation of imidacloprid in industrial water by GC-MS and LC-MS. *Analysis* **1998,** *26* (7), 245-251.
25. Navalón, A.; González-Casado, A.; El-Khattabi, R.; Vílchez, J. L.; Fernández-Alba, A. R., Determination of imidacloprid in vegetable samples by gas chromatography–mass spectrometry. *Analyst* **1997,** *122* (6), 579-581.
26. Guiberteau, A.; Galeano, T.; Mora, N.; Parrilla, P.; Salinas, F., Study and determination of the pesticide Imidacloprid by square wave adsorptive stripping voltammetry. *Talanta* **2001,** *53* (5), 943-949.
27. Guzsvány, V. J.; Gaál, F. F.; Bjelica, L. J.; Ökrész, S. N., Voltammetric determination of imidacloprid and thiamethoxam. *Journal of the Serbian Chemical Society* **2005,** *70* (5), 735-743.
28. Li, L.; Jiang, G.; Liu, C.; Liang, H.; Sun, D.; Li, W., Clothianidin dissipation in tomato and soil, and distribution in tomato peel and flesh. *Food Control* **2012,** *25* (1), 265-269.
29. Papp, Z.; Guzsvány, V.; Svancara, I.; Vytras, K., Carbon paste electrodes for the analysis of some agricultural pollutants and trace metals. *Journal of Agricultural Science and Technology* **2011,** *5* (1), 85-92.
30. Ví lchez, J. L.; Valencia, M. C.; Navalón, A.; Molinero-Morales, B.; Capitán-Vallvey, L. F., Flow injection analysis of the insecticide imidacloprid in water samples with photochemically induced fluorescence detection. *Analytica Chimica Acta* **2001,** *439* (2), 299-305.
31. Lovera, P.; Creedon, N.; Alatawi, H.; Mitchell, M.; Burke, M.; Quinn, A. J.; O'Riordan, A., Low-cost silver capped polystyrene nanotube arrays as super-hydrophobic substrates for SERS applications. *Nanotechnology* **2014,** *25* (17), 175502.
32. Albrecht, M. G.; Creighton, J. A., Anomalously intense Raman spectra of pyridine at a silver electrode. *Journal of the American Chemical Society* **1977,** *99* (15), 5215-5217.
33. Fleischmann, M.; Hendra, P. J.; McQuillan, A. J., Raman spectra of pyridine adsorbed at a silver electrode. *Chemical Physics Letters* **1974,** *26* (2), 163-166.
34. Otto, A.; Mrozek, I.; Grabhorn, H.; Akemann, W., Surface-enhanced Raman scattering. *Journal of Physics: Condensed Matter* **1992,** *4* (5), 1143.
35. Stiles, P. L.; Dieringer, J. A.; Shah, N. C.; Duyne, R. P. V., Surface-Enhanced Raman Spectroscopy. *Annual Review of Analytical Chemistry* **2008,** *1* (1), 601-626.
36. Creedon, N. C.; Lovera, P.; Furey, A.; O'Riordan, A., Transparent polymer-based SERS substrates templated by a soda can. *Sensors and Actuators B: Chemical* **2018,** *259*, 64-74.
37. Becke, A. D., Density-functional thermochemistry. III. The role of exact exchange. *The Journal of chemical physics* **1993,** *98* (7), 5648-5652.

38. Weigend, F.; Ahlrichs, R., Balanced basis sets of split valence, triple zeta valence and quadruple zeta valence quality for H to Rn: Design and assessment of accuracy. *Physical Chemistry Chemical Physics* **2005,** *7* (18), 3297-3305.
39. Ma, C.; Zaino III, L. P.; Bohn, P. W., Self-induced redox cycling coupled luminescence on nanopore recessed disk-multiscale bipolar electrodes. *Chemical science* **2015,** *6* (5), 3173-3179.
40. Grimme, S., Semiempirical GGA-type density functional constructed with a long-range dispersion correction. *Journal of computational chemistry* **2006,** *27* (15), 1787-1799.
41. Peng, C.; Ayala, P. Y.; Schlegel, H. B.; Frisch, M. J., Using redundant internal coordinates to optimize equilibrium geometries and transition states. *Journal of Computational Chemistry* **1996,** *17* (1), 49-56.
42. Deglmann, P.; Furche, F.; Ahlrichs, R., An efficient implementation of second analytical derivatives for density functional methods. *Chemical physics letters* **2002,** *362* (5-6), 511-518.
43. Deglmann, P.; Furche, F., Efficient characterization of stationary points on potential energy surfaces. *The Journal of Chemical Physics* **2002,** *117* (21), 9535-9538.
44. Merrick, J. P.; Moran, D.; Radom, L., An evaluation of harmonic vibrational frequency scale factors. *The Journal of Physical Chemistry A* **2007,** *111* (45), 11683-11700.
45. Khaikin, L. S.; Grikina, O. E.; Lokshin, B. V.; Dyugaev, K. P.; Astakhov, A. M., Vibrational spectra of 1,1,3,3-tetramethyl-2-nitroguanidine and their interpretation with the use of scaling of quantum-chemical force field. *Russian Chemical Bulletin* **2008,** *57* (3), 499-505.
46. Zhang, F.; Zhang, Y.; Ni, H.; Ma, K.; Li, R., Experimental and DFT studies on the vibrational, electronic spectra and NBO analysis of thiamethoxam. *Spectrochimica Acta Part A: Molecular and Biomolecular Spectroscopy* **2014,** *118*, 162-171.
47. Jalkanen, J.-P.; Zerbetto, F., Interaction model for the adsorption of organic molecules on the silver surface. *The Journal of Physical Chemistry B* **2006,** *110* (11), 5595-5601.
48. Sackmann, M.; Materny, A., Surface enhanced Raman scattering (SERS)—a quantitative analytical tool? *Journal of Raman Spectroscopy: An International Journal for Original Work in all Aspects of Raman Spectroscopy, Including Higher Order Processes, and also Brillouin and Rayleigh Scattering* **2006,** *37* (1-3), 305-310.
49. Socrates, G., *Infrared and Raman Characteristic Group Frequencies: Tables and Charts*. John Wiley & Sons: 2001.
50. Zhu, X.-M.; Zhang, S.-Q.; Zheng, X.; Phillips, D. L., Resonance Raman study of short-time photodissociation dynamics of the charge-transfer band absorption of nitrobenzene in cyclohexane solution. *The Journal of Physical Chemistry A* **2005,** *109* (13), 3086-3093.
51. Markham, L. M.; Mayne, L. C.; Hudson, B. S.; Zgierski, M. Z., Resonance Raman studies of imidazole, imidazolium, and their derivatives: the effect of deuterium substitution. *The Journal of Physical Chemistry* **1993,** *97* (40), 10319-10325.
52. Sundaraganesan, N.; Ilakiamani, S.; Anand, B.; Saleem, H.; Joshua, B. D., FTIR, FT-Raman spectra and ab initio DFT vibrational analysis of 2-amino-5-chloropyridine. *Spectrochimica Acta Part A: Molecular and Biomolecular Spectroscopy* **2006,** *64* (3), 586-594.
53. Kumar, M.; Srivastava, M.; Yadav, R. A., Vibrational studies of benzene, pyridine, pyridine-N-oxide and their cations. *Spectrochimica Acta Part A: Molecular and Biomolecular Spectroscopy* **2013,** *111*, 242-251.
54. Chen, L.; Gao, Y.; Xu, H.; Wang, Z.; Li, Z.; Zhang, R.-Q., The mechanism of N-Ag bonding determined tunability of surface-enhanced Raman scattering of pyridine on MAg (M = Cu, Ag, Au) diatomic clusters. *Physical Chemistry Chemical Physics* **2014,** *16* (38), 20665-20671.
55. Lin-Vien, D.; Colthup, N. B.; Fateley, W. G.; Grasselli, J. G., *The handbook of infrared and Raman characteristic frequencies of organic molecules*. Elsevier: 1991.
56. European Food Safety Authority, The 2011 European Union Report on Pesticide Residues in Food. *EFSA Journal 2014* **2014,** *12* (5), 3694.

57. Li, M.; Sheng, E.; Cong, L.; Wang, M., Development of Immunoassays for Detecting Clothianidin Residue in Agricultural Products. *Journal of Agricultural and Food Chemistry* **2013,** *61* (15), 3619-3623.
58. Kim, B. M.; Park, J.-S.; Choi, J.-H.; Abd El-Aty, A. M.; Na, T. W.; Shim, J.-H., Residual determination of clothianidin and its metabolites in three minor crops via tandem mass spectrometry. *Food Chemistry* **2012,** *131* (4), 1546-1551.
59. Papp, Z.; Švancara, I.; Guzsvány, V.; Vytřas, K.; Gaál, F., Voltammetric determination of imidacloprid insecticide in selected samples using a carbon paste electrode. *Microchim Acta* **2009,** *166* (1-2), 169-175.
60. Obana, H.; Okihashi, M.; Akutsu, K.; Kitagawa, Y.; Hori, S., Determination of Neonicotinoid Pesticide Residues in Vegetables and Fruits with Solid Phase Extraction and Liquid Chromatography Mass Spectrometry. *Journal of Agricultural and Food Chemistry* **2003,** *51* (9), 2501-2505.
61. Chen, M.-F.; Huang, J.-W.; Wong, S.-S.; Li, G.-C., Analysis of insecticide clothianidin and its metabolites in rice by liquid chromatography with a UV detector. *Journal of Food and Drug Analysis* **2005,** *13* (3), 279-283.
62. Guzsvány, V.; Papp, Z.; Zbiljić, J.; Vajdle, O.; Rodić, M., Bismuth Modified Carbon-Based Electrodes for the Determination of Selected Neonicotinoid Insecticides. *Molecules* **2011,** *16* (6), 4451.
63. Kashid, L.; Pawar, N., Voltammetric behaviour of imidacloprid and its electrochemical mineralization assessment by differential pulse polarography. *International Journal of Scientific and Research Publications* **2015**.
64. Kumaravel, A.; Chandrasekaran, M., Electrochemical determination of imidacloprid using nanosilver Nafion®/nanoTiO2 Nafion® composite modified glassy carbon electrode. *Sensors and Actuators B: Chemical* **2011,** *158* (1), 319-326.
65. Navalón, A.; El-Khattabi, R.; González-Casado, A.; Vilchez, J., Differential-pulse polarographic determination of the insecticide imidacloprid in commercial formulations. *Microchim Acta* **1999,** *130* (4), 261-265.
66. Kong, L.; Jiang, X.; Zeng, Y.; Zhou, T.; Shi, G., Molecularly imprinted sensor based on electropolmerized poly(o-phenylenediamine) membranes at reduced graphene oxide modified electrode for imidacloprid determination. *Sensors and Actuators B: Chemical* **2013,** *185* (0), 424-431.
67. Brycht, M.; Vajdle, O.; Zbiljić, J.; Papp, Z.; Guzsvány, V.; Skrzypek, S., Renewable Silver-Amalgam Film Electrode for Direct Cathodic SWV Determination of Clothianidin, Nitenpyram and Thiacloprid Neonicotinoid Insecticides Reducible in a Fairly Negative Potential Range. *International Journal of Electrochemical Science* **2012,** *7* (11).
68. Hou, R.; Pang, S.; He, L., In situ SERS detection of multi-class insecticides on plant surfaces. *Analytical Methods* **2015,** *7* (15), 6325-6330.
69. Zhang, H.; Kang, Y.; Liu, P.; Tao, X.; Pei, J. W.; Li, H.; Du, Y. P., Determination of Pesticides by Surface-Enhanced Raman Spectroscopy on Gold-Nanoparticle-Modified Polymethacrylate. *Analytical Letters* **2016,** *49* (14), 2268-2278.

Table of Contents Graphic